Earth Surf. Dynam., 6, 451–466, 2018
https://doi.org/10.5194/esurf-6-451-2018

Earth Surface Dynamics
Open Access
EGU

On the Holocene evolution of the Ayeyawady megadelta

Liviu Giosan[1], Thet Naing[2], Myo Min Tun[3], Peter D. Clift[4], Florin Filip[5], Stefan Constantinescu[6], Nitesh Khonde[1,7], Jerzy Blusztajn[1], Jan-Pieter Buylaert[8], Thomas Stevens[9], and Swe Thwin[10]

[1]Geology & Geophysics, Woods Hole Oceanographic, Woods Hole, USA
[2]Department of Geology, Pathein University, Pathein, Myanmar
[3]Department of Geology, University of Mandalay, Mandalay, Myanmar
[4]Geology & Geophysics, Louisiana State University, Baton Rouge, USA
[5]The Institute for Fluvial and Marine Systems, Bucharest, Romania
[6]Geography Department, Bucharest University, Bucharest, Romania
[7]Birbal Sahni Institute of Palaeosciences, Lucknow, India
[8]DTU Nutech, Center for Nuclear Technologies, Technical University of Denmark, Roskilde, Denmark
[9]Department of Earth Sciences, Uppsala University, Uppsala, Sweden
[10]Department of Marine Science, Mawlamyine University, Mawlamyine, Myanmar

Correspondence: Liviu Giosan (lgiosan@whoi.edu)

Received: 12 November 2017 – Discussion started: 20 November 2017
Revised: 27 February 2018 – Accepted: 1 May 2018 – Published: 12 June 2018

Abstract. The Ayeyawady delta is the last Asian megadelta whose evolution has remained essentially unexplored so far. Unlike most other deltas across the world, the Ayeyawady has not yet been affected by dam construction, providing a unique view on largely natural deltaic processes benefiting from abundant sediment loads affected by tectonics and monsoon hydroclimate. To alleviate the information gap and provide a baseline for future work, here we provide a first model for the Holocene development of this megadelta based on drill core sediments collected in 2016 and 2017, dated with radiocarbon and optically stimulated luminescence, together with a reevaluation of published maps, charts and scientific literature. Altogether, these data indicate that Ayeyawady is a mud-dominated delta with tidal and wave influences. The sediment-rich Ayeyawady River built meander belt alluvial ridges with avulsive characters. A more advanced coast in the western half of the delta (i.e., the Pathein lobe) was probably favored by the more western location of the early course of the river. Radiogenic isotopic fingerprinting of the sediment suggests that the Pathein lobe coast does not receive significant sediment from neighboring rivers. However, the eastern region of the delta (i.e., Yangon lobe) is offset inland and extends east into the mudflats of the Sittaung estuary. Wave-built beach ridge construction during the late Holocene, similar to several other deltas across the Indian monsoon domain, suggests a common climatic control on monsoonal delta morphodynamics through variability in discharge, changes in wave climate or both. Correlation of the delta morphological and stratigraphic architecture information on land with the shelf bathymetry, as well as its tectonic, sedimentary and hydrodynamic characteristics, provides insight on the peculiar growth style of the Ayeyawady delta. The offset between the western Pathein lobe and the eastern deltaic coast appears to be driven by tectonic–hydrodynamic feedbacks as the extensionally lowered shelf block of the Gulf of Mottama amplifies tidal currents relative to the western part of the shelf. This situation probably activates a perennial shear front between the two regions that acts as a leaky energy fence. Just as importantly, the strong currents in the Gulf of Mottama act as an offshore-directed tidal pump that helps build the deep mid-shelf Mottama clinoform with mixed sediments from the Ayeyawady, Sittaung and Thanlwin rivers. The highly energetic tidal, wind and wave regime of the northern Andaman Sea thus exports most sediment offshore despite the large load of the Ayeyawady River.

1 Introduction

Asian megadeltas (Woodroffe et al., 2006) have a long history of human habitation and anthropogenic impact. With large populations, which increasingly congregate in sprawling megacities, these vast low-lying and ecologically rich regions are under threat from environmental degradation, climate change and sea level rise. The Ayeyawady (formerly known as Irrawaddy) is the least studied of these megadeltas despite its scientific, social and economic importance (Hedley et al., 2010). Located in the larger India–Asia collision zone, the Ayeyawady delta (Fig. 1) bears the imprint of uniquely complex tectonic processes in a region of oblique subduction (Morley et al., 2007) and is a repository for unusually large sediment yields under an erosion-prone monsoon climate (e.g., Giosan et al., 2017). Sediment redistribution within the delta and on the shelf fronting is affected by strong tides amplified by the geomorphology of the region (Ramasawamy and Rao, 2014). In contrast to other Asian megadeltas, the Ayeyawady River basin is arguably less transformed by post-World War II anthropogenic impacts, although humans have probably affected delta development since at least the Iron Age as agriculture expanded along the river (Moore, 2007) and later intensified during the Pyu ($\sim$ 200 BC to 1050 AD), Bagan ($\sim$ 850 to 1300 AD) and Ava ($\sim$ 1350 to 1550 AD) historical periods. Recent rapid development trends and population growth underline the need to understand the history and document the current state of the Ayeyawady delta.

Although the Ayeyawady River is less regulated compared to other large rivers, plans are afoot to construct several dams across it and this may change the water and sediment regimes, as well as fluxes reaching its low-lying delta plain (Brakenridge et al., 2017). Inundation of the Ayeyawady delta region during the cyclone Nargis in 2008 was one of the costliest and deadliest natural disasters ever recorded (Fritz et al., 2009; Seekins, 2009). Catastrophic monsoon-driven river floods are also common and devastating (Brakenridge et al., 2017). The Ayeyawady delta may already be sediment deficient (Hedley et al., 2010) and the anticipated sediment deficit after damming could increase its vulnerability to such transient events as well as to long-term sea level rise (Giosan et al., 2014). Strong tidal currents in the northern Andaman Sea (Rizal et al., 2012) amplify some aspects of delta vulnerability, such as salinization (Taft and Evers, 2016), whereas other aspects such as sediment redistribution along the coast or sediment trapping within the subaerial delta (e.g., Hoitink et al., 2017) may be attenuated. Better knowledge on how the delta has formed and functioned will help future efforts to maintain its viability.

To alleviate the information gap and provide a baseline for future work, here we sketch a first model for the Holocene evolution of the Ayeyawady delta based on new field data collected in two expeditions in 2016 and 2017 (Figs. 2 and 3; see Fig. S1 in the Supplement for site locations and names) together with a reevaluation of published maps, charts and scientific literature (Figs. 4 and 5). In the process we reassess our knowledge concerning monsoonal deltas in general by advancing new ideas on how morphodynamics and sedimentary architecture can be controlled by feedbacks between tectonics and tides as well as by the balance between fluvial discharge and wave climate.

2 Background

The Ayeyawady River is a major fluvial system that became individualized in the Oligocene–early Miocene time (Fig. 1; Licht et al., 2016; Morley, 2017, and references therein). The Upper Cretaceous subduction of the Neotethys Ocean followed by the collision between India and Asia first led to an Andean-type margin comprised of the Wuntho–Popa volcanic arc and associated forearc and back-arc basins (e.g., Lee et al., 2006; Racey and Ridd, 2015; Liu et al., 2016). The uplift of the Indo-Burman Ranges accretionary prism since the early Paleogene completed the separation of the Central Myanmar Basin (CMB) from the Bay of Bengal. The complex of basins forming the CMB were further segmented by compression and inversion (e.g., Bender, 1983). These basins include the Ayeyawady Valley separated by the Bago Yoma (Pegu Yoma) from the Sittaung (Sittang) Valley flowing along the Shan Plateau. The Ayeyawady River infilled this $\sim$ 900 km long shallow marine area toward the Andaman Sea, a Cenozoic back-arc and strike-slip basin induced by oblique subduction of the Indian plate under Eurasia (e.g., Curray, 2005). A southern shift in Ayeyawady deposition was evident in the Miocene after the strike-slip Sagaing fault activated along Bago Yoma. The Holocene delta is the last realization in a series of deltas comprising this southward-moving Ayeyawady depocenter.

Myanmar's hydroclimate that is responsible for Ayeyawady flow is spatially complex owing to its varied topography and compound influences from both the Indian and East Asian monsoon systems (Brakenridge et al., 2017). Orographic precipitation occurs along the northeastern Himalayas and Indo-Burman Ranges (Xie et al., 2006), as well as the Shan Plateau feeding the upper Ayeyawady and the Chindwin, whereas central Myanmar, on the leeward side of these ranges, remains drier. The upper basin of the Ayeyawady also receives snow and glacier meltwater in the spring. Over 90 % of the discharge at the delta occurs between May and October with small but significant interannual variability (Furuichi et al., 2009) linked to the El Niño–Southern Oscillation, Indian Ocean dipole and Pacific Decadal Oscillation (D'Arigo and Ummenhofer, 2014, and references therein).

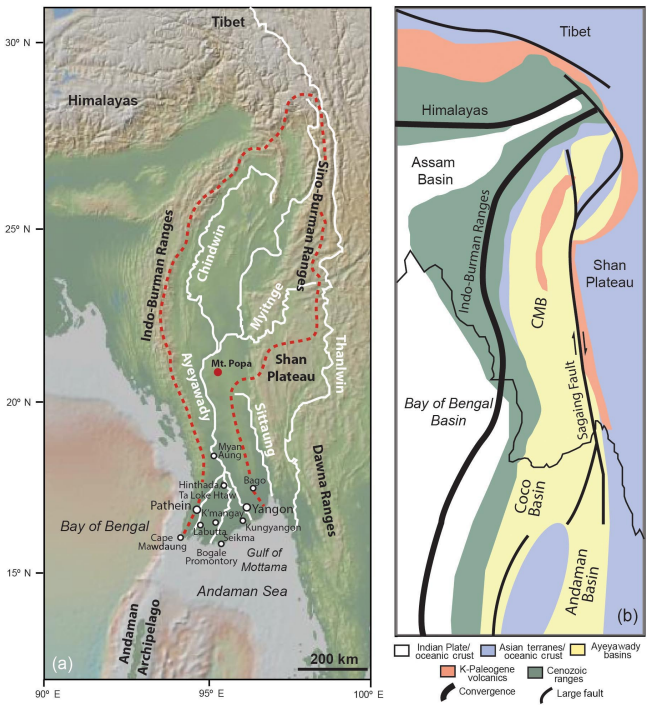

Figure 1. **(a)** Physiography and **(b)** geology of the Ayeyawady basin and adjacent regions.

In historical times the Ayeyawady River has transported $\sim 422 \pm 41 \times 10^9$ m^3 of freshwater every year to the ocean (Robinson et al., 2007), watering Myanmar from north to south along the way (Fig. 1). The water discharge apparently decreased to the present level of $379 \pm 47 \times 10^9$ m^3 yr^{-1} (Furuichi et al., 2009). Among the delta-building Himalayan rivers, the Ayeyawady is a prodigious sediment conveyor ($\sim 364 \pm 60 \times 10^6$ t yr^{-1}), second only to the combined Ganges–Brahmaputra (Robinson et al., 2007). Between 40 and 50 % of the sediment comes from the upper Ayeyawady with the rest supplied by its main tributary, the Chindwin (Garzanti et al., 2016). Sediments transported by the upper Ayeyawady River come primarily from erosion of gneisses and granitoids of the eastern Himalayan syntaxis region and the Sino-Burman Ranges. Although draining less steep terrain, the Chindwin contributes more sediment than the upper Ayeyawady from the easily erodible flysch and low-grade metasedimentary rocks of the Indo-Burman Ranges. Both water and sediment discharge vary synchronously at interannual timescales as a function of monsoon intensity (Furuichi et al., 2009), but they have changed little since the late 19th century when Gordon (1893) measured them systematically for the first time. In addition to the Ayeyawady, the Sittaung River supplies sediment to the northern shore of the Gulf of Mottama (aka the Gulf of Martaban) where its estuary merges with the Ayeyawady delta coast (Fig. 1). The sediment discharge from the Sittaung is unknown but can be estimated based on its annual water discharge range from 50×10^9 m^3 to a maximum of 40 to 50×10^6 t yr^{-1} by assuming sediment yields similar to the Ayeyawady's (Milliman and Farnsworth, 2010). Another sediment contributor to the Gulf of Mottama ($\sim 180 \times 10^6$ t yr^{-1}; Robinson et al., 2007) is the Thanlwin River (Salween) draining the eastern Shan Plateau and eastern Tibetan Plateau. Information about the variability in Ayeyawady's sediment discharge over the Holocene lifetime of the delta is sparse, as are reconstructions for the monsoon regime in its basin. Assuming the modern direct correlation between water discharge and sediment load, one may qualitatively infer an increase in sediment delivery since 10 000 years ago with a peak at around 5000 years ago when the Andaman Sea was at its freshest (Gebregeorgis et al., 2016), followed by a decrease to the present values, as the Indian monsoon has weakened since the early Holocene (e.g., Ponton et al., 2012).

The Ayeyawady delta is a mud-dominated delta that exhibits mainly tidal and secondarily wave influences (Figs. 2 and 5; Kravtsova et al., 2009). Ayeyawady's single braided channel starts to show avulsive behavior near the town of Myanaung ($\sim 18.2°$ N) where the tidal influence is still felt ~ 290 km from the Andaman Sea (Fig. 1). The apex of the delta, defined as the region of deltaic distributary bifurcation, is north of the town of Hinthada (18° N) around 270 km from the coast. Multiple branches are active in the delta, splitting and rejoining to form a network of higher-order distributary channels and reaching the coast through 11 tidally enlarged estuaries (Fig. 2). Most of the water discharge (76 %) is delivered to the Andaman Sea through three main mouths: Pyamalaw, Ayeyawady and To-Thakutpin from west to east (Kravtsova et al., 2009).

In natural conditions when the delta was covered by tropical forests and mangroves (Adas, 2011), sedimentation on the delta plain occurred within active and abandoned channels, on channel levees, and in inter-distributary basins (Stamp, 1940; Kravtsova et al., 2009). The coast prograded via shoal/bar emergence and wave-built beach ridges with associated inter-ridge swales (Kravtsova et al., 2009). The coastline for the Ayeyawady delta proper stretches from the western rocky Cape Mawdaung (formerly Pagoda Point), adjacent to the Pathein River, to the Yangon River in the east (Fig. 1). However, this conventional definition does not capture the fact that the accumulative coast with sediment input from the Ayeyawady continues east of Yangon River into the Sittaung estuary. Despite the large fluvial sediment load of the combined Ayeyawady and Sittaung delivered annually ($350–480 \times 10^6$ t), shoreline changes have been puzzlingly minor along the Ayeyawady delta coast since 1850 (Hedley et al., 2010). Sea level change data are sparse and unreliable for the delta and no data on subsidence or uplift exist.

The shelf morphology in front of the Ayeyawady delta is complex due to its tectonic structure and the nature of Holocene sedimentation (Rodolfo, 1969a, b, 1975; Ramaswamy and Rao, 2014). The width of the shelf is ~ 170 km wide off the Ayeyawady River mouths, widening

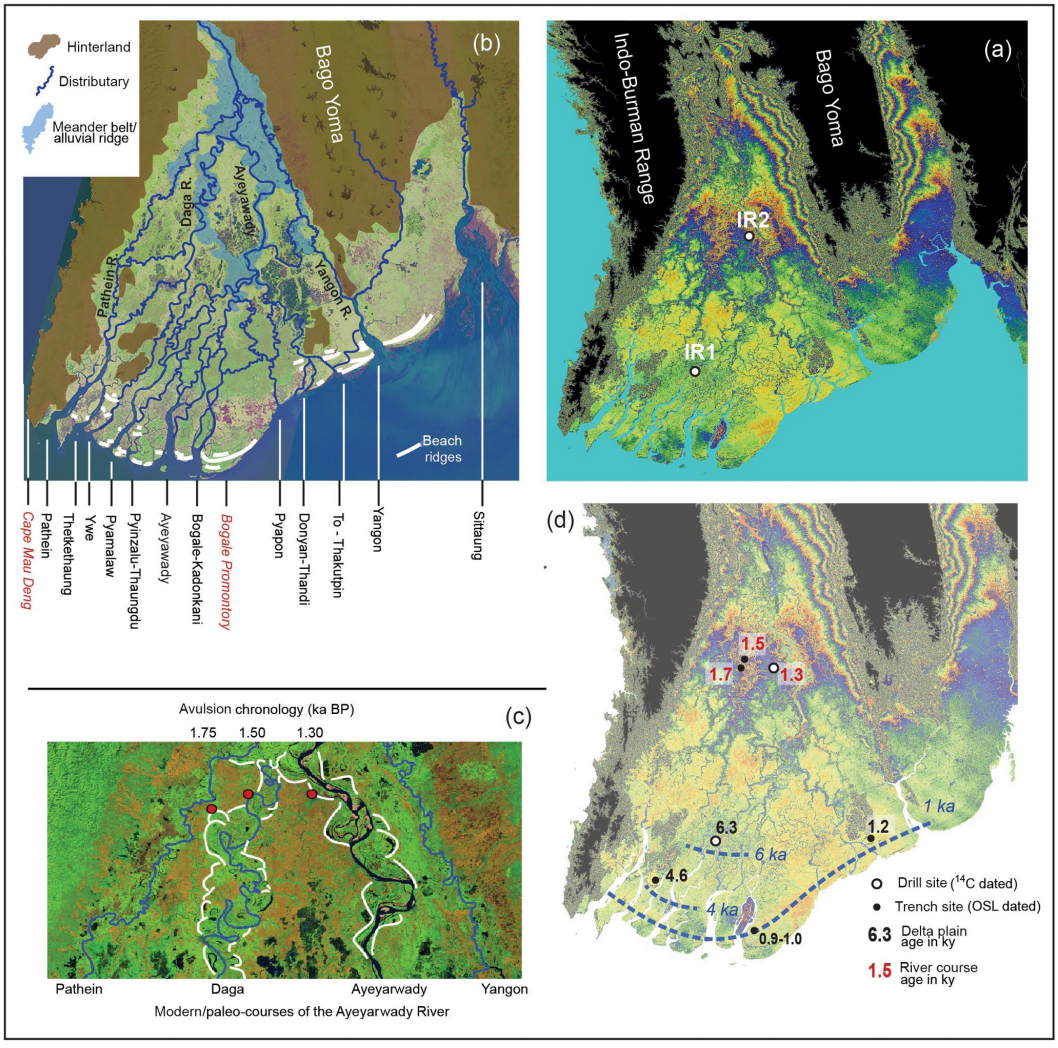

Figure 2. **(a)** SRTM-derived DEM for the Ayeyawady delta region (pattern of colors repeats every 10 to 300 m in height; higher land in black); **(b)** large-scale features of the Ayeyawady delta region with identified river and distributary courses and mouths as well as beach ridges shown on an ASTER satellite photo; **(c)** sample locations and chronology on the meander belts documenting the avulsion near the delta apex (meander belts as white lines delimited from ASTER and Google Earth images); **(d)** preliminary model of the Ayeyawady delta evolution with sampling locations and types with chronological information on the youngest fluvial deposits and beach ridges.

to more than 250 km in the Gulf of Mottama (Figs. 1 and 5). The shelf edge exhibits a flat, platform-like indentation in the Gulf of Mottama between 140 and 180 m deep (i.e., the Martaban depression – Ramaswamy and Rao, 2014) that features a dendritic network of channels feeding the Martaban Canyon (Rodolfo, 1975). Most of the large Ayeyawady sediment suspended load is redistributed by the strong tidal currents (Fig. 5) and seasonally reversing wind currents to be deposited on the wide northern Andaman shelf (Ramaswamy and Rao, 2014) where it mixes with sediment from the Sittaung, Thanlwin and other smaller rivers (Damodararao et al., 2016). Semidiurnal tides vary between 2 and 3 m from the Pathein River to the Bogale River, reaching higher stages inside distributaries. The tidal range is gradually amplified to macrotidal conditions on the shallow (< 30 m) shelf of the Gulf of Mottama from the Bogale promontory toward the Sittaung estuary where it reaches above 7 m during spring tides (British Admiralty, 1935). Associated tidal currents also vary accordingly to over 3.5 m s^{-1} near the Sittaung mouth.

Waves are subordinate in importance to tides, with average heights of less than 1 m in winter to 1–2 m in summer (Kravtsova et al., 2009). Tidal currents combine with the wind-driven circulation. Wind currents are clockwise during the summer monsoon and reversed during the winter monsoon (Rizal et al., 2012). The macrotidal regime maintains turbid conditions year-round with the turbidity front oscillating ∼ 150 km in the Gulf of Mottama in phase with the spring–neap tidal cycle (Ramaswamy et al., 2004). An-

nual turbidity levels and suspended sediment distribution are modulated by the monsoonal-driven winds, currents and river discharge (Ramaswamy et al., 2004; Matamin et al., 2015), with the most extensive and compact turbid waters occurring in boreal winter. During the summer the turbidity region shrinks to the Gulf of Mottama and nearshore regions where river plumes are active and dispersed eastward. Turbidity profiles show an increase with depth during fair weather and uniform concentrations during major storms or cyclones (Ramaswamy et al., 2004; Shi and Wang, 2008). Bottom nepheloid layers and possibly hyperpycnal flows occur in the Gulf of Mottama and flow into the interior of the Andaman Sea as mid-water nepheloid layers (Ramaswamy et al., 2004).

The bathymetric characteristics of the shelf and the circulation system favor deposition of fine fluvial sediments in a mud belt that widens from the western edge of the Ayeyawady coast into the Gulf of Mottama that more or less coincides in extent with the high-turbidity region (Ramaswamy and Rao, 2014). The outer shelf, including the Martaban depression, is a zone of low to non-deposition, and exhibits a relict morphology with topographic irregularities that host relict coarsely grained carbonate-rich sediment and fauna with patchy Holocene muds (Ramaswamy and Rao, 2014).

In terms of human impacts on the delta, it is important to note that the population of Myanmar increased from 4–5 million in the late 19th century to $\sim$51 million in 2014 with 30 % residing in the Ayeyawady delta region. This large increase in population not only led to a rapid rate of deforestation in the basin but also to destruction of mangroves for agriculture and fuel in the delta (Taft and Evers, 2016). An earlier large migration wave to the delta occurred in the latter half of the 19th century when the British colonial authorities cleared much of the delta forests and mangroves for rice agriculture (Adas, 2011). Construction of dikes to protect agricultural lands in the delta began in 1861 and continued aggressively until the 1920s. These dikes are generally of a horseshoe type protecting delta islands in the upstream and sides from the flood wave, but recently poldering with diking entire islands was employed. Most channels remain natural with no extensive system of dredged canals. However, all dikes limit overbank flooding and deposition of sediment (Volker, 1966; Stamp, 1940) and the entire agricultural system favors salinization of soils in the delta. The model for the Holocene evolution of the Ayeyawady delta that we provide below allows us to assess first-order relationships to the complex regional tectonics, climate and shelf circulation as a baseline for the future development and management of the delta.

3 Methods

The large-scale morphology of the Ayeyawady delta, together with the adjoining regions (Fig. 2), was assessed and studied using satellite data and old maps of the region. High-resolution (90 m) digital elevation data were derived from NASA's Shuttle Radar Topography Mission (SRTM; Farr et al., 2007). Digital elevation models (DEMs) were constructed at 300 m resolution and were used in combination with the Advanced Spaceborne Thermal Emission and Reflection Radiometer (ASTER) and Google Earth to identify geomorphic features that provide insight into fluvial morphodynamics. The delta and upstream floodplain were delimited from adjacent hinterlands with associated marginal alluvial fans, as were remnant inselberg-like pre-deltaic terrains inside the delta. We identified active and abandoned river courses and delta distributaries and their meander belts. Finally, we identified fossil beach ridges denoting former delta shorelines. Guided by this assessment, in two field expeditions in the Ayeyawady delta in 2016 and 2017, we collected sedimentary records from shallow hand-dug trenches and cores with mechanized pneumatic and percussion drilling (Figs. 2 and 3; see also Fig. S1).

Fossil wave-built beach ridges were targeted by trenching in order to obtain a chronology for the delta coast advance (Figs. 1 and 2; see also Fig. S1). Samples for optically stimulated luminescence (OSL) dating were collected where possible from within the beach–foreshore facies in watertight opaque tubes (site I-11 at Labutta in the western part of the delta, sites I-12 and I-13 at Seikma near the central delta coast, and site I-14 at Kungyangon near the eastern delta coast). A sample was collected in the anthropogenic overburden to date habitation on a Labutta beach ridge (site I-10). In addition, two levee samples were collected on meanders of the now defunct western major branch of the Ayeyawady (Figs. 1 and 2; Table 2) near the apex of the delta (i.e., sites I-8 near Ta Loke Htaw and I-9 near Lemyethna bordering the last abandoned course and an earlier-formed oxbow lake, respectively). Levee samples were collected in trenches at the top of each levee, below the overburden.

Drill coring was designed to recover continuous sediment records to the pre-deltaic Pleistocene sediments (Figs. 2 and 3; see also Fig. S1; Table 1). Drill sites were located in the middle and near the apex of the delta (core IR1 to 70.4 m of depth at Kyonmangay located 6.7 m above sea level (m a.s.l.) and core IR2 to 43 m of depth at Ta Loke Htaw located at 18 m a.s.l.) to assess the deltaic architecture and, in particular, how far the postglacial transgression reached inside the suspected Pleistocene Ayeyawady incised valley. Facies analysis was based on the visual description of lithology, sedimentary structures, textures and benthic foraminifera presence. In addition, X-ray-fluorescence-scanning high-resolution chemostratigraphy was employed for the drill cores to identify depositional environments using the Itrax X-ray fluorescence scanner of Woods Hole Oceanographic Institution (WHOI) (see methodology in Croudace et al., 2006). From the suite of measured elements we used the [Si] / [Rb] ratio to characterize the sand content (i.e., Si-rich sand relative to finely grained muds, rich in Rb; Croudace

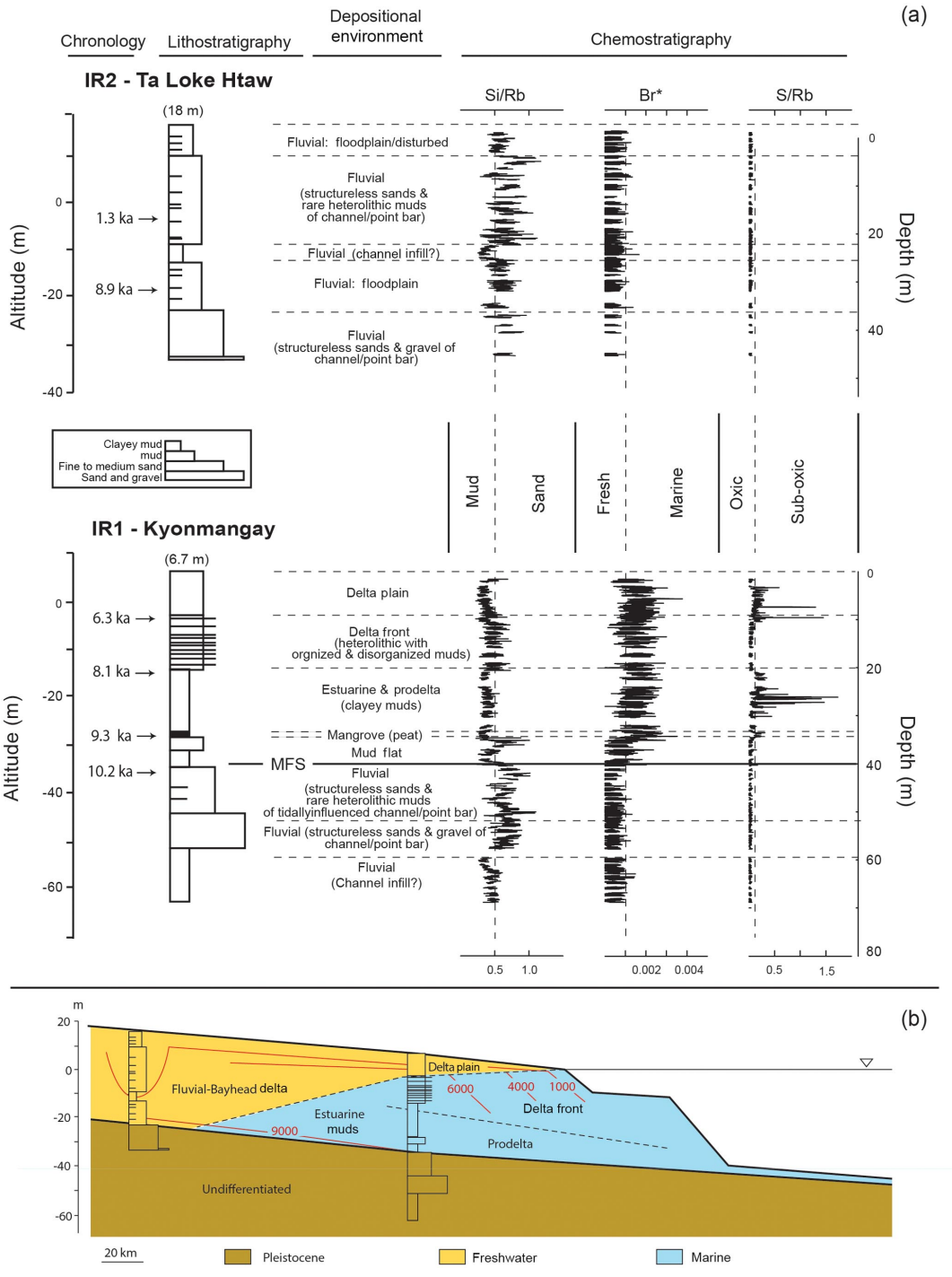

Figure 3. **(a)** Depositional environments interpreted from litho- and chemo-stratigraphy with radiocarbon chronology for drill cores in the Ayeyawady delta; **(b)** interpreted Ayeyawady delta stratigraphy and evolution along the Ayeyawady's main course.

and Rothwell, 2015), the [Br] / [total X-ray fluorescence counts] ratio or Br* to characterize the organic matter (i.e., with Br enriched in marine organic matter; McHugh et al., 2008) and the [S] / [Rb] ratio to characterize redox conditions in finely grained muds (i.e., with S in excess of terrigenous values in reducing conditions; Croudace and Rothwell, 2015).

Sediment sources for the pre-modern delta were estimated using radiogenic isotopes (Nd and Sr) on a bulk sediment sample from the delta apex trench (I-8 taken as representative for Ayeyawady fluvial sediment). To assess any poten-

Table 1. Results of AMS ^{14}C dating of organic materials from drill cores IR1 (Kyonmangay) and IR2 (Ta Loke Htaw).

Location	Sample	Altitude (m b.s.l.)	Type	Lab code	Latitude	Longitude	Age (years BP)	Error (years BP)	δ^{13}C (‰)	Calibrated age (years)*	Error (years)	Observations
Kyonmangay	IR1-9.60	−2.9	leaf fragment	OS-132754	16°26′15″ N	95°08′01″ E	5590	100	−28.65	6487	213	small
Kyonmangay	IR1-20.0	−13.3	leaf fragment	OS-132658	16°26′15″ N	95°08′01″ E 7300	40	−26.71	8166	80		
Kyonmangay	IR1-35.0	−28.3	mangrove wood piece	OS-133490	16°26′15″ N	95°08′01″ E	8300	40	−27.27	9352	148	
Kyonmangay	IR1-40.0	−33.3	carbonized wood piece	OS-132659	16°26′15″ N	95°08′01″ E	9100	35	−26.58	10351	88.5	
Ta Loke Htaw	IR2-19.0	−0.5	wood trunk piece	OS-133606	17°39′13″ N	95°26′2″ E	1320	15	−28.04	1307	53.5	
Ta Loke Htaw	IR2-33.5	−15.0	carbonized wood piece	OS-135132	17°39′13″ N	95°26′2″ E	8020	30	−27.7	8959	117.5	small

* Calendar ages are relative to the year 2016.

tial addition of non-Ayeyawady sediment sources (e.g., littoral drift, marine biogenic carbonates) another pre-modern sample from the youngest dated fossil beach ridge trench near the coast (I-12) was measured both as bulk and decarbonated. The radiogenic composition of sediments from Sittaung River, the closest source to the delta other than the Ayeyawady itself, was measured in a floodplain sample near Bago (Fig. 1). Nd and Sr chemistry was undertaken with conventional ion chromatography following the method of Bayon et al. (2002). Strontium was separated and purified from samples using Sr-Spec (Eichrom) resin. Nd chemistry was performed with Ln resin (Eichrom) following the method described in Scher and Delaney (2010). Sr and Nd analyses were conducted on the NEPTUNE multi-collector inductively coupled plasma mass spectrometry (ICP-MS) at WHOI with the internal precision around 10–20 ppm (2σ); external precision, after adjusting $^{87}Sr/^{86}Sr$ and $^{143}Nd/^{144}Nd$ values by 0.710240 and 0.511847 for the SRM987 and La Jolla Nd standards, respectively, is estimated to be 15–25 ppm (2σ).$^{143}Nd/^{144}Nd$ isotopic composition is expressed further as εNd (DePaolo and Wasserburg, 1976) units relative to $(^{143}Nd/^{144}Nd)CHUR = 0.512638$ (Hamilton et al., 1983).

Plant and wood pieces were radiocarbon-dated to derive a chronology for the deltaic sediment succession and the predeltaic base (Table 1). Accelerator mass spectrometry (AMS) radiocarbon dating was performed at the National Ocean Sciences Accelerator Mass Spectrometry (NOSAMS) facility at the WHOI. The methodology for AMS radiocarbon dating is presented on the NOSAMS site (www.whoi.edu/nosams, last access: 28 May 2018) and discussed in McNichol et al. (1995). All dates have been converted to calendar ages using CalPal 4.3 (Bronk Ramsey, 2009) and the IntCal13 calibration dataset (Reimer et al., 2013).

Seven samples were collected for OSL dating. Samples were collected using lighttight metal tubes hammered horizontally into cleaned sediment surfaces. The tubes were opened under subdued orange light at the Nordic Laboratory for Luminescence Dating (Aarhus University) located at Risø (DTU Nutech) in Denmark. Using standard sample preparation techniques (wet sieving, acid treatment, heavy liquids) purified quartz and K-feldspar-rich extracts in the 180–250 µm grain size range were obtained (except sample 177 202 for which it was 90–180 µm). Multigrain aliquots of quartz and K feldspar were measured using a single-aliquot regenerative-dose (SAR) protocol (Murray and Wintle, 2000) suitable for young samples. The purity of the quartz OSL signal was confirmed using an OSL infrared (IR) depletion ratio test (Duller, 2003; all aliquots within 10 % of unity). For quartz OSL preheating for dose and test dose was performed at 200°C for 10 s and 160°C for 0 s, respectively. K-feldspar-rich extracts were measured using a post-IR infrared stimulated luminescence (IRSL) (pIRIR150) protocol based on Madsen et al. (2011). Early and late background subtraction was used for quartz OSL and feldspar pIRIR dose

calculations, respectively. Total dose rates to quartz and K feldspar were calculated from radionuclide concentrations measured on the outer material from the tubes using high-resolution gamma-ray spectrometry (Murray et al., 1987). Samples were assumed to have been saturated with water throughout the entire burial lifetime.

The morphology of the subaqueous extension of the Ayeyawady delta was studied using the only available detailed bathymetric chart of the region that was based on surveys from 1850 to 1929 with small corrections until 1935 (British Admiralty, 1935). Newer navigation charts of the region report only small corrections afterwards. The final DEM (Figs. 4 and 5) consists of 6442 individual soundings reduced to the original datum at Elephant Point at the entrance in Yangon River; to these we added the digitized bathymetric contours of the original chart. To extend the bathymetry offshore beyond the coverage of the original chart we used the GEBCO 2014 Grid (General Bathymetric Charts of the Oceans, a global 30 arcsec interval grid). Prior to digitizing, all charts and satellite photos used in this study were georeferenced and transformed to a common UTM projection (Zone 46° N WGS84) with Global Mapper 18.0 (http://www.globalmapper.com/, last access: 28 May 2018) using 16 control points for each chart or photo. DEMs at a 250 m spatial resolution were generated from digitized soundings with Surfer 12.0 software (Golden Software, Inc.). The "natural neighbor" algorithm was chosen for interpolation because it is suitable for a variable density of data across the interpolation domain and does not extrapolate depth values beyond the range of existing data.

4 Results

In concert with satellite photos, our SRTM DEM (Fig. 2a) reveals that the morphologically defined Ayeyawady delta plain starts immediately after the river emerges from its mountainous valley at Myanaung, bound on the western side by the Indo-Burma Range and massive alluvial fans originating in the Bago Yoma on the eastern side. Several inselberg-like pre-deltaic high terrains occur close to the coast on the western side of the Pathein River and on both sides of the Yangon River. Two alluvial ridges, 5 to 7 m high relative to their adjacent delta plain, with visible meander belts and rare crevasse splays, were constructed by large trunk channels (Fig. 2a, b, c). The western alluvial ridge along the Daga course is largely fossil, whereas the eastern ridge is being built along the present course of the river (Fig. 2c). Both ridges taper off in the mid-delta as the trunk channels start to bifurcate into distributaries that split and rejoin on the lower delta (Fig. 2a, b). After the bifurcation zone the delta plain is uniformly low in altitude (< 5 m) with the exception of the higher mudflats near the entrance in the Sittaung estuary (Fig. 2a). Although possessing meander belts of their own in their upper reaches, the Pathein and Yangon rivers, located at the western and eastern edges of the delta, do not show visibly large alluvial ridges (Fig. 2a, b), suggesting that they were not preferential routes for the main trunk of the Ayeyawady but secondary courses, or they have not been active for very long. Near the coast, several generations of wave-built beach ridges are evident in the lower part of the delta, bundling occasionally into beach ridge plains on the Bogale promontory and on the sides of the Yangon River (Fig. 2b).

Sediment in our trenches on the Ayeyawady beach ridges exhibited weakly stratified, mud-rich, fine sand lithologies. Fluvial deposits trenched near the apex showed a typical levee facies exhibiting weakly laminated, amalgamated fine sands and muds below the bioturbated and human-disturbed overburden. The IR1 drill core (Fig. 3) at Kyonmangay (Fig. 2; see also Fig. S1) shows a succession of delta plain bioturbated soils and delta plain muds overlaying amalgamated fine to medium sand and muds of the delta front and prodelta/estuarine clayey muds with intercalated organic-rich detritus layers. Marine influences are documented in the prodelta/estuarine and delta front deposits by high Br* values and rare benthic foraminifers. Tidal influence is indicated by thick–thin and sand–mud alternations in the delta front deposits. Flooding is suggested by occasional clean sandy layers in the prodelta facies. Both the delta plain and prodelta/estuarine deposits show increased S / Rb values, indicating poorly oxic conditions. The transition to delta front advance at Kyonmangay occurred at 13.5 m below sea level (m b.s.l.) ∼ 8100 years ago, as documented by the radiocarbon content of a leaf fragment. The deltaic succession stands on a 9300-year-old mangrove peat at 28.5 m b.s.l. near the base of the deltaic Holocene deposits. Pre-Holocene fluvial deposits older than 10 200 years BP occur below, consisting of structureless medium to coarse sands with clayey mud intercalations, gravels and finely grained weakly laminated channel infills.

The IR2 drill core (Fig. 3) at Ta Loke Htaw (Fig. 2; see also Fig. S1) near the delta apex on the modern alluvial ridge exhibits a succession of delta plain sandy muds topping structureless medium sands with rare intercalated thin muds of channel/point bar type. They overlie finely grained, weakly laminated channel infill deposits and fine floodplain sands with intercalated thin muds that started to accumulate ∼ 8900 years BP (radiocarbon-dated wood piece). Below ∼ 25 m b.s.l. structureless fine to medium sands of channel/point bar and gravel layers occur to the base of the drill core. Organic material is rare in all facies at Ta Loke Htaw except for occasional wood branches and a tree trunk in the upper point bar facies. Marine influence is absent as foraminifers are not encountered and Br* levels are consistently low.

The quartz OSL and feldspar pIRIR150 luminescence dating results are summarized in Tables 2 and S1. The quartz OSL signal is dominated by the fast component and the average dose recovery ratio is 1.00 ± 0.02 (four samples, 11–

Table 2. Summary of the quartz and feldspar luminescence data. (*n*) denotes the number of aliquots contributing to dose (De). The saturated water content (w.c.) is given as the ratio of the weight of water to dry sediment weight. Feldspar IR50 and pIRIR150 ages have not been corrected for any signal instability. Radionuclide concentrations used to derive quartz and feldspar dose rates are given in Table S1. Bleaching of quartz OSL signal is assessed by comparing the quartz ages with the IR50 and pIRIR150 ages. Uncertainties represent 1 standard error. Age uncertainties include random and systematic components. Quartz ages should be used for interpretation; feldspar ages are only used to investigate quartz OSL bleaching.

						Quartz		Quartz	pIRIR$_{150}$		IR$_{50}$	Quartz		pIRIR$_{150}$	IR$_{50}$	Quartz		K feldspar	
Sample code			Site	Setting	Latitude/longitude	Depth, cm	well-bleached?	Age, ka	Age, ka	Age, ka	Age, ka	Dose, Gy	(*n*)	Dose, Gy	(*n*)	Dose rate, Gy ka^{-1}	Dose rate, Gy ka^{-1}	Dose rate, Gy ka^{-1}	w.c. %
17	72	01	I8	fluvial levee	17 38 36.82 N/ 95 18 33.64 E	95	probably	1.50 ± 0.23	6.64 ± 0.68	1.20 ± 0.23	3.28 ± 0.49	34	20.6 ± 1.9	3.73 ± 0.69	9	2.19 ± 0.10	3.10 ± 0.12	29
17	72	02	I9	fluvial levee	17 36 13.5 N/ 95 12 53.39 E	110	not certain	1.75 ± 0.32	15.2 ± 5.5	4.02 ± 1.85	4.14 ± 0.73	35	46 ± 16	12.0 ± 5.5	9	2.37 ± 0.10	2.99 ± 0.11	35
17	72	03	I10	beach ridge	16 09 03.5 N/ 94 43 57.3 E	92	probably	1.46 ± 0.22	2.35 ± 0.21	1.10 ± 0.07	2.97 ± 0.42	40	6.9 ± 0.5	3.25 ± 0.17	9	2.03 ± 0.09	2.95 ± 0.11	28
17	72	04	I11	beach ridge	16 09.2578 N/ 94 44.1843 E	90	confident	4.63 ± 0.47	4.73 ± 0.37	2.71 ± 0.17	10.1 ± 0.9	36	14.7 ± 1.0	8.42 ± 0.43	9	2.18 ± 0.09	3.10 ± 0.11	32
17	72	05	I12	beach ridge	15 50 10.5 N/ 95 29 51 E	100	probably	1.04 ± 0.09	1.94 ± 0.19	0.79 ± 0.05	2.64 ± 0.17	38	6.7 ± 0.6	2.72 ± 0.14	9	2.53 ± 0.13	3.45 ± 0.15	38
17	72	06	I13	beach ridge	15 49.6494 N/ 95 30.2095 E	132	probably	0.86 ± 0.07	1.86 ± 0.15	0.68 ± 0.04	1.58 ± 0.12	37	5.1 ± 0.4	1.88 ± 0.08	9	1.84 ± 0.07	2.75 ± 0.10	40
17	72	07	I14	beach ridge	16 24 27.5 N/ 96 02 20.2 E	115	probably	1.19 ± 0.11	1.43 ± 0.12	0.76 ± 0.04	2.64 ± 0.19	40	4.5 ± 0.3	2.38 ± 0.09	9	2.21 ± 0.10	3.13 ± 0.12	24

12 aliquots per sample), suggesting that our quartz De values measured using SAR are reliable. One prerequisite for accurate age estimation is that the quartz OSL signal was sufficiently bleached prior to burial in the sediment sequence. In this study we use the feldspar IR50 and pIRIR150 age data to provide insights into the completeness of bleaching of the quartz OSL signal (e.g., Murray et al., 2012; Rémillard et al., 2016). This is based on the observation that feldspar signals bleach much more slowly than quartz OSL (Godfrey-Smith et al., 1988; Thomsen et al., 2008): IR50 signals bleach approximately 1 order of magnitude slower than quartz OSL, and pIRIR signals bleach even more slowly than IR50 signals (e.g., Kars et al., 2014; Colarossi et al., 2015). We are confident that the quartz signal is well bleached when the pIRIR150 age agrees within uncertainty with the quartz age; this is the case for sample 177 204. We consider that the quartz OSL signal is very likely to be completely bleached when the IR50 age agrees or is slightly lower (due to fading) than the quartz age. This is the case for all samples except for sample 177 202, for which the IR50 age may be slightly older. Nevertheless, this does not mean the quartz OSL age for this particular sample is affected by partial bleaching; we just cannot be certain it is not.

Overall, optical ages on the natural levee of an oldest meander series of the eastern fossil alluvial ridge indicate full activity by $\sim 1750 \pm 320$ years ago. Sedimentation on the top of the natural levee bordering the last Daga course indicate that its abandonment took place no earlier than 1500 ± 230 years ago (Fig. 2; see also Fig. S1). A radiocarbon date calibrated to ~ 1300 years ago on a large wood trunk from the point bar facies drilled at Ta Loke Htaw indicates that the present eastern course of the Ayeyawady was active at the time. The fresh appearance of the wood makes it unlikely that it is remobilized fossil wood. However, a future systematic exploration of the meander belts' subsurface architecture is needed to reconstruct their history.

Our combined chronology indicates the Ayeyawady delta reached as far south as the latitude of the cities of Yangon and Pathein around 6300 years ago, as documented by the radiocarbon content of a leaf fragment from the delta plain facies at Kyonmangay. Optical dating shows that the least advanced beach ridge bundle found on the western side of the delta near Labutta is also the oldest (~ 4600 years old; Figs. 2 and S1). The beach ridge plain at the Bogale promontory started ~ 1000 years ago, soon after beach ridges started to form at the Yangon River mouth (~ 1200 years ago; Figs. 2 and S1).

Radiogenic provenance fingerprinting of the bulk river sediment (Table S2) on the Ta Loke Htaw levee shows $^{143}Nd/^{144}Nd$ (εNd) and $^{87}Sr/^{86}Sr$ values of 0.512263 (-7.3) and 0.7120, respectively, close to the beach ridge sediment composition: 0.512285 (-6.9) and 0.7118 for bulk sediment and 0.512287 (-6.8) and 0.7119 for bulk decarbonated sediment. The identical $^{87}Sr/^{86}Sr$ values for the bulk and decarbonated beach ridge sample suggest that marine

biogenic carbonates are a minor sediment component at the coast. However, previous measurements on Ayeyawady sediments (Table S2 with data from Allen et al., 2008 – 150 km upstream of the delta; Colin et al., 1999 – at an unspecified location) show a larger variability in εNd with values of −8.3 and −10.7. The closest sediment source along the coast, the Sittaung River that drains Bago Yoma and the Shan Plateau shows $^{143}Nd/^{144}Nd$ (εNd) and $^{87}Sr/^{86}Sr$ values of 0.512105 (−10.4) and 0.7168, respectively. The Yangon River, the largely abandoned easternmost branch of the Ayeyawady close to Bago Yoma, has εNd and $^{87}Sr/^{86}Sr$ of −12.2 and 0.7080, respectively (Damodararao et al., 2016), which suggest mixing with a source similar to Sittaung.

Our reassessment of the late 19th–early 20th century bathymetry with the high-resolution DEM produced several surprises (Figs. 3 and 4a). First, the edge of the shelf (Fig. 4) was found to be significantly deeper in front of the Mottama depression (> 150 m) then west of it (100–120 m deep). Second, the mud belt along the Ayeyawady delta exhibits a clinoform attached to the shore and likely composed of sandy muds (Rao et al., 2005) and extending to depths of 35–40 m. In contrast, the Gulf of Mottama exhibits a thick mid-shelf clinoform probably comprised of finer muds (Rao et al., 2005) with the steep frontal region extending from 40 to 90 m of water depth. The transition between the western and eastern clinoforms is marked by a transversal channel that is 10 km wide and 5 m deep on average and is flanked on the deeper eastern side by a drift-like elongated feature of similar average dimensions. Third, a flatter area of the outer shelf in front of the western Ayeyawady delta coast stands out from the typical outer-shelf chaotic relief, suggesting potential preservation of a relict pre-Holocene delta region at water depths between 35 and 45 m.

5 Discussion

Our new drill core information (Fig. 3) indicates that the Ayeyawady delta advanced into an incised valley estuarine embayment that extended north of Kyonmangay (∼ 80 km from the current coast) but did not reach as far as the current delta apex at Ta Loke Htaw (270 km from the coast). The Pleistocene deposits of the incised valley intercepted in our cores are fluvial, generally much coarser than the delta deposits but heterolithic, with indications of increasing tidal influence nearer to the Andaman Sea at Kyonmangay. The overlying peats atop mudflat sediments sampled at Kyonmangay indicate the presence of a muddy coast with mangroves at the time of their transgression ∼ 9300 years ago. Given that the contemporaneous ice-volume equivalent global sea level was between −29 and −31 m b.s.l. (Lambeck et al., 2014), the altitude of the mangrove peat (−28.3 m b.s.l.) on the largely incompressible Pleistocene deposits below indicate that the delta is vertically stable. However, glacial isostatic adjustment modeling is needed to quantify subsidence as neighboring regions of Thailand and the Malay Peninsula (Bradley et al., 2016) suggest that the relative sea level reached higher earlier during the deglaciation. After the mangrove coast was flooded, the marine embayment accumulated estuarine and prodelta muds afterwards. About 8100 years ago the Ayeyawady bayhead delta front reached the southern Kyonmangay site and by ∼ 6300 years ago delta plain deposition had started.

Deposits at the delta apex in the drill core at Ta Loke Htaw indicate a dynamic fluvial environment with channel erosion (i.e., scouring) followed by point bar and floodplain deposition. The abandonment of the western Daga meander belt not much after 1500 years ago suggests that the Ayeyawady started to flow on a single preferential course close to that time. Meander belt construction on the old and new course of the river, leading to the formation of alluvial ridges, appears to be an efficient type of aggradation on the upper delta plain before the river starts to bifurcate.

Near the coast, the quasi-contemporary beach ridge development on the Bogale promontory and Yangon River mouth suggest that the advanced position of the western half of the delta was acquired early and maintained during progradation. Delta growth since 6300 years ago, with intermediate stages delineated by successive beach ridge sets, suggest decreasing rates of advance of $\sim 25\,m\,yr^{-1}$ until ∼ 4600 years ago and 8 to $10\,m\,yr^{-1}$ afterwards. The latter are still higher than the average progradation value of $3.4\,m\,yr^{-1}$ calculated by Hedley et al. (2010) for the last century or so. Furthermore, the recent progradation occurred primarily on the coast adjacent to both sides of the Yangon River, while the shoreline of the rest of the delta has been largely immobile.

It is important to note that, like the Ayeyawady, many large river deltas developing under the Asian monsoon regime, such as the Mekong (Ta et al., 2002), Red River (Tanabe et al., 2003) or Godavari (Cui et al., 2017), started to form wave-built beach ridges between 5000 and 4000 years ago, changing from river-dominated morphologies to show stronger wave-influenced characteristics. Given that these deltas were at various stages of advance from within their incised valleys onto the shelf, it is more likely that their morphological evolution was climatically driven rather than controlled by local factors as previously proposed. As the late Holocene monsoon aridification started at that time (Ponton et al., 2012), fluvial discharge variability at centennial timescales increased, setting the stage for periodic wave dominance of deltaic coasts during more arid intervals.

Our reevaluation of the shelf morphology in the context of the new data on land reveals important information for understanding the peculiar, irregular growth of the Ayeyawady delta with its western half from Cape Mawdaung to the Bogale promontory well advanced into the Andaman Sea in comparison to its eastern half. First, the shelf DEM suggests that the western Ayeyawady delta continues offshore into a shallow, shore-attached clinoform, which is not completely unexpected given the relatively low tidal range of 2–3 m (e.g.,

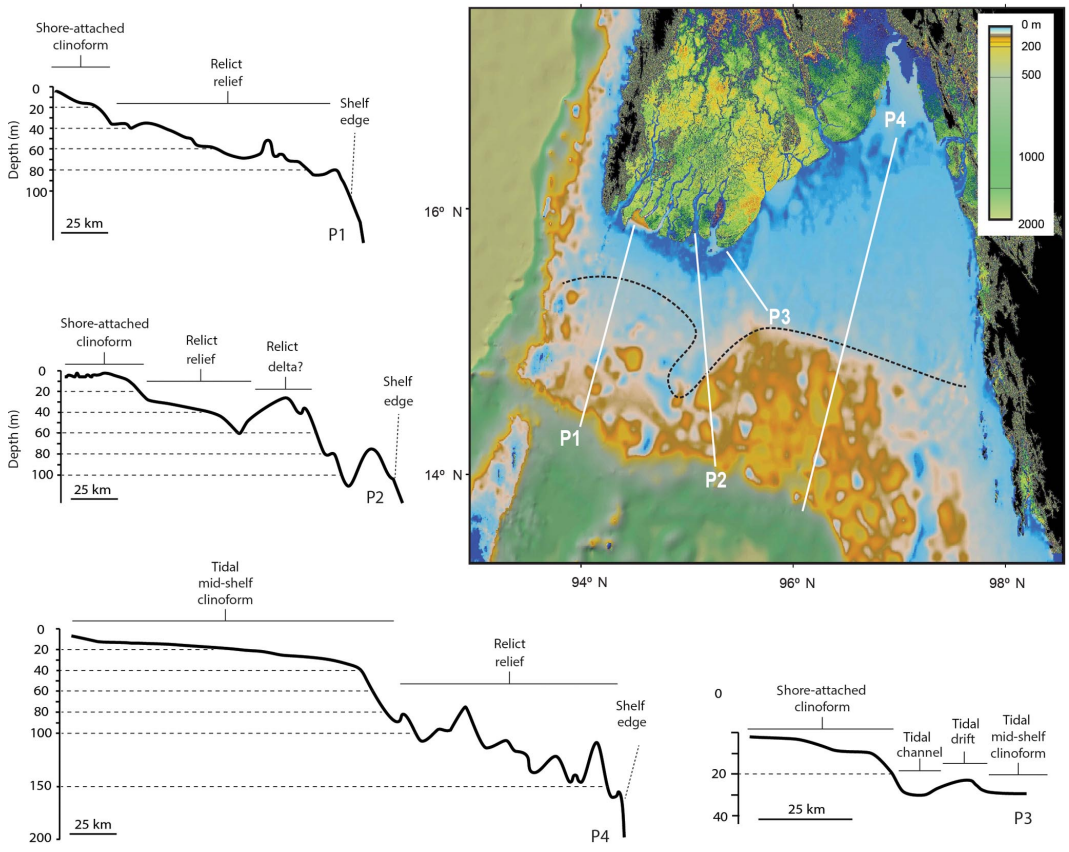

Figure 4. Interpreted bathymetric profiles across the northern Andaman Sea shelf (bathymetric profiles identified on map). Dashed line on map indicates the approximate limit of consistent finely grained sediment deposition on the shelf farthest from shore. The SRTM-derived DEM for the Ayeyawady delta region is shown on land.

Goodbred and Saito, 2012) and the perennial loss of sediment advected to the Gulf of Mottama (Ramaswamy and Rao, 2014). The Nd and Sr fingerprint of the river sediment is almost identical to the beach ridge at Bogale, indicating that essentially no sediment from the Gulf of Mottama bearing the radiogenic imprint of Sittaung (see above) and especially Thanlwin (Damodararao et al., 2016) is feeding this part of the coast. The shore-attached sandy clinoform tapers off after 40 m b.s.l. (Fig. 2b). In contrast, the Gulf of Mottama exhibits a mid-shelf mud clinoform with the rollover at 40 m and a toe depth of 80–90 m. The internal architecture of this distinctive feature was imaged previously (Ramaswamy and Rao, 2014), showing seismic characteristics typical of a clinoform topset and foreset. High rates of progradation and aggradation for the Mottama clinoform have been previously suggested but a core collected on its lower foreset has an average sedimentation rate of $\sim 1\,\mathrm{cm\,yr^{-1}}$ since ~ 1450 AD (Ota et al., 2017), which is 1 order of magnitude less than proposed before (Chhibber, 1934; Rodolfo, 1975). Given the depressed character of the Mottama shelf indicated by the shelf edge position 40 to 70 m lower than in front of the western Ayeyawady delta, it is not surprising that infilling of this region is still ongoing. What is surprising instead is why and how the Ayeyawady River built its delta on the eastern raised shelf block rather than advancing preferentially into the Gulf of Mottama defying theoretical and modeling expectations of a more advanced deltaic coast toward the subsided block (e.g., Liang et al., 2016). The key to this problem appears to be again suggested by the shelf morphology.

The distinctive transition between clinoforms exhibiting a wide elongated channel and what appears to be an attached sediment drift-like feature suggests intense current activity at the common boundary between the two clinoforms. Indeed, tidal modeling suggests that a tidal shear front (e.g., Wang et al., 2017) may be present in this region that shows a drastic change from weak and more isotropic tidal currents west of Bogale promontory to highly oriented strong currents in the Gulf of Mottama (Rizal et al., 2012). Such a shear front would explain both the unusual channel–drift couplet and the fact that the Ayeyawady was able to build its delta west of the gulf. If the tidal shear front has been a long-lived feature of the shelf circulation it probably acted as a littoral energy fence (sensu Swift and Thorne, 1992) trapping a significant part of the Ayeyawady coarser sediment on the raised western shelf block. However, such an energy fence may be broken by prevailing westerly currents during

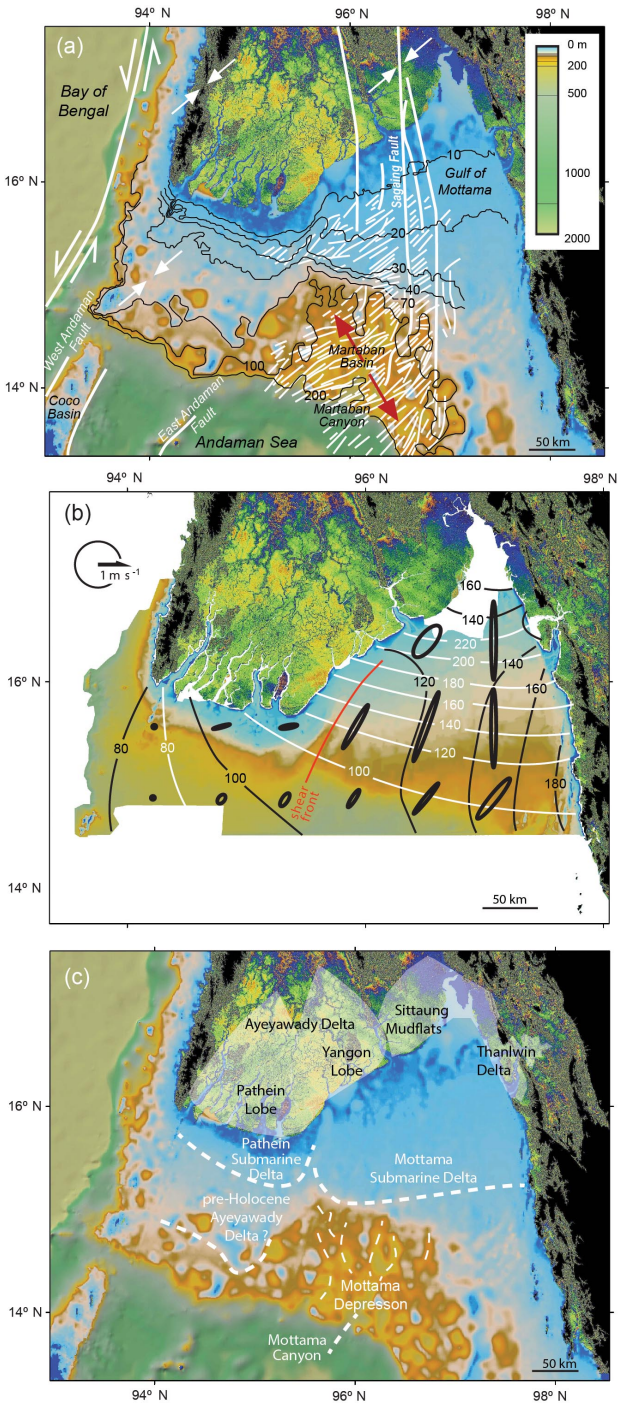

Figure 5. **(a)** Bathymetry of the northern Andaman Sea shelf and SRTM-derived DEM for the Ayeyawady delta region on land with regional faults and associated splay faults (Morley, 2007); arrow pairs indicate regional compression (white) or extension (red); **(b)** tidal range lines (black), cotidal lines (white) and tidal current magnitudes (ellipses) for the dominant M2 tide component (Rizal et al., 2012); **(c)** sketch of the Ayeyawady delta plain evolution phases and associated subaqueous deltas.

the summer monsoon when water and sediment discharge from the Ayeyawady peaks to provide suspended sediment to the Mottama clinoform. Given the depressed character of the Mottama shelf block, the front must have existed since the beginning of the deglacial transgression of the northern Andaman shelf. Industrial seismic reflection profiles imaged a region of strike-slip extension in the Gulf of Mottama expressed as horsetail extensional splays linked to the Sagaing fault system (Morley, 2007) that can explain the height differential between the western and eastern shelves. Furthermore, the shear front must have gradually intensified through positive feedback with the morphology as the shore-attached clinoform west of it grew larger. In contrast, the amplified tidal currents in the Gulf of Mottama efficiently redistributed the significantly larger amount of Ayeyawady sediment that escaped beyond the energy fence together with sediments from Sittaung and Thanlwin to form the mid-shelf clinoform there. The offshore-directed tidal pumping leading to the formation of the Mottama clinoform is reminiscent of the situation on the eastern Indus shelf where strong tidal currents from the Gulf of Kutch built a mid-shelf clinoform with Indus sediments escaping eastward (Giosan et al., 2006). Such clinoforms, which are of purely tidal origin and do not front a subaerial deltaic counterpart per se, may have been more common in sediment-rich macrotidal environments during faster transgressive conditions in the past.

6 Conclusions

The Ayeyawady delta in Myanmar is the last realization in a long series of depocenters that gradually moved southward within the tectonically dynamic intra-mountainous landscape extending from the Central Myanmar Basin in the north to the northern Andaman Sea in the south (Figs. 1 and 2). The delta appears to be vertically stable within the incised valley dug by the Ayeyawady River during the last low stand (Fig. 3). The Pleistocene valley was flooded at least 80 km inland from the present coast during the deglacial sea level rise. Holocene progradation into this paleo-Ayeyawady bay proceeded in the form of a fluvial- and tide-dominated delta until late Holocene wave action began to build isolated and clustered beach ridges at the contemporaneous coasts (Fig. 2). However, beach ridges are rather rare and underdeveloped, testifying to the enormous sediment load discharged by the Ayeyawady and tidal dispersal and reworking. Ridge construction during the late Holocene, similar to several other deltas across the Indian monsoon domain, suggests a possible climatic control on delta morphodynamics through variability in discharge, changes in wave climate or both.

The landscape near the delta apex exhibits active and late Holocene fossil meander belts that terminate in the mid-delta where the discharge is split to lower-order distributary channels (Fig. 2). The meander belts stand as alluvial ridges above the floodplain along the active river course, as well as its an-

tecedent paleo-course documenting the Ayeyawady's avulsive character. Construction of a more advanced coast in the western half of the delta could be seen as a quasi-independent region, the Pathein lobe (Fig. 5), which was probably favored by the more western location of the early course of the river (but see below). The eastern region of the delta (the Yangon lobe) is offset inland (Fig. 5) and exhibits a more wave-dominated morphology, largely built with Ayeyawady-derived sediment escaping alongshore. Further east, the Yangon lobe merges with the mudflats fringing the Sittaung estuary (Fig. 5). Despite its large sediment load the Thanlwin River has only built a bayhead delta, barely prograding outside its incised valley, probably due to extreme macrotidal conditions at its mouth (Fig. 5). However, its sediment contributed instead to deposition on the shelf, as did most of the load from both the Ayeyawady and Sittaung.

Correlation of the delta morphological and stratigraphic architecture information on land to the shelf bathymetry and hydrodynamics, as well as its tectonic and sedimentary characteristics, provides insight on the peculiar growth style of the Ayeyawady delta (Figs. 2–5). The offset between the western Pathein lobe and the eastern deltaic coast appears to be driven by tectonic–hydrodynamic feedbacks as the extensionally lowered shelf block of the Gulf of Mottama amplifies tidal currents relative to the eastern part of the shelf. This situation probably activates a perennial shear front between the two regions that acts as a leaky energy fence. Just as importantly, the strong currents in the Gulf of Mottama act as an offshore-directed tidal pump that help build a deep, mixed-source mid-shelf clinoform, the Ayeyawady–Sittaung–Thanlwin subaqueous delta, into the Mottama shelf depression.

Our study takes a first look at the evolution of the Holocene Ayeyawady delta to provide a basis for more detailed work and context to present future management plans for this ecologically and economically important, but vulnerable, region. A first conclusion for the future of the region comes by comparing the Ayeyawady to other deltas across the world. Uniquely for deltas of its size the Ayeyawady delta has not suffered a sediment deficit from damming, yet it has been barely growing. The reason is the highly energetic tidal, wind and wave regime of the northern Andaman Sea that exports most sediments offshore despite the large load of the river, as described by Ramswamy et al. (2004) and Hedley et al. (2010). In addition to their effects upstream (Brakenridge et al., 2017), the expected sediment deficit after dams are constructed on the river and tributaries may significantly impact the fragile delta sedimentary equilibrium (Giosan et al., 2014) rendering it more vulnerable to the accelerating sea level rise (Syvitski et al., 2009) or changes in frequency and intensity of cyclones hitting the coast (Darby et al., 2016) compounded with increased subsidence linked to the rapid development of the region (e.g., Van der Horst, 2017).

Data availability. The text herein and Supplement contain all data discussed in this paper.

The Supplement related to this article is available online at https://doi.org/10.5194/esurf-6-451-2018-supplement.

Competing interests. The authors declare that they have no conflict of interest.

Acknowledgements. This study was primarily supported by an Andrew W. Mellon Foundation Award for Innovative Research from the Woods Hole Oceanographic Institution to Liviu Giosan. Additional funds were provided by the Charles T. McCord Chair in Petroleum Geology to Peter D. Clift. We thank Myanmar authorities for project permissions as well as leaders and residents of villages that we visited in the Ayeyawady delta for hospitality and help. We also thank Venkitasubramani Ramaswamy (NIO, Goa) for providing inspiration with his previous Andaman Sea work and for help with initial contacts in Myanmar. Nitesh Khonde gratefully acknowledges the SERB Indo-U.S. Postdoctoral Fellowship sponsored by SERB-IUSSTF for research work at Woods Hole Oceanographic Institution, USA.

Edited by: Daniel Parsons
Reviewed by: Kelvin Rodolfo and Torbjörn Törnqvist

References

Adas, M.: The Burma Delta: Economic Development and Social Change on an Asian Rice Frontier, 1852–1941, New Perspectives in SE Asian Studies, Univ. of Wisconsin Press, 2011.

Allen, R., Najman, Y., Carter, A., Barfod, D., Bickle, M. J., Chapman, H. J., Garzanti, E., Vezzoli, G., Andò, S., and Parrish, R. R.: Provenance of the Tertiary sedimentary rocks of the Indo-Burman Ranges, Burma (Myanmar): Burman arc or Himalayan-derived?, J. Geol. Soc., 165, 1045–1057, 2008.

Bayon, G., German, C. R., Boella, R. M., Milton, J. A., Taylor, R. N., and Nesbitt, R. W.: An improved method for extracting marine sediment fractions and its application to Sr and Nd isotopic analysis, Chem. Geol., 187, 179–199, 2002.

Bender, F.: Geology of Burma, Gebrüder Borntraeger, Berlin, 1983.

Bradley, S. L., Milne, G. A., Horton, B. P., and Zong, Y.:, Modelling sea level data from China and Malay-Thailand to estimate Holocene ice-volume equivalent sea level change, Quaternary Sci. Rev., 137, 54–68, 2016.

Brakenridge, G. R., Syvitski, J. P. M., Nieburh, E., Overeem, I., Higgins, S. A., Kettner, A. J., and Prades, L.: Design with nature: causation and avoidance of catastrophic flooding, Myanmar, Earth-Sci. Rev., 165, 81–109, 2017.

British Admiralty: Bay of Bengal, East Coast, Sheet III, Coronge Island to White Point, including the Gulf of Martaban, British Admiralty, 1935.

Bronk Ramsey, C.: Bayesian analysis of radiocarbon dates, Radiocarbon, 51, 337–360, 2009.

Chhibber, H. L.: The Geology of Burma, Macmillan, London, 1934.

Colarossi, D., Duller, G. A. T., Roberts, H. M., Tooth, S., and Lyons, R.: Comparison of paired quartz OSL and feldspar post-IR IRSL dose distributions in poorly bleached fluvial sediments from South Africa, Quat. Geochronol., 30, 233–238, 2015.

Colin, C., Turpin, L., Bertraux, J., Desprairies, A., and Kissel, C.: Erosional history of the Himalayan and Burman ranges during the last two glacial–interglacial cycles, Earth Planet. Sc. Lett., 171, 647–660, 1999.

Croudace, I. W. and Rothwell, R. G.: Micro-XRF Studies of Sediment Cores, Dev. Paleoenviron. Res., 17, Springer, 2015.

Croudace, I. W., Rindby, A., and Rothwell, R. G. ITRAX: description and evaluation of a new X-ray core scanner, in: New Techniques in Sediment Core Analysis, edited by: Rothwell, R. G., Geol. Soc. Lond. Spec. Publ., 267, 51–63, 2006.

Cui, M., Wang, Z., Nageshwara Rao, K., Sangode, S. J., Saito, Y., Chen, T., Kulkarni, Y. R., Ganga Kumar, K. C., and Demudu, V.: A mid-to-late Holocene record of vegetation decline and erosion triggered by monsoon weakening and human adaptations in the south–east Indian Peninsula, Holocene, 27, 1976–1987, 2017.

Curray, J. R.: Tectonics of the Andaman Sea region, J. Asian Earth Sci., 25, 187–232, 2005.

D'Arrigo, R. and Ummenhofer, C. C.: The climate of Myanmar: evidence for effects of the Pacific Decadal Oscillation, Int. J. Climatol., 35, 634–640, https://doi.org/10.1002/joc.3995, 2014.

Damodararao K., Singh S. K., Rai V. K., Ramaswamy, V., and Rao, P. S.: Lithology, Monsoon and Sea-Surface Current Control on Provenance, Dispersal and Deposition of Sediments over the Andaman Continental Shelf, Front. Mar. Sci., 3, 118, https://doi.org/10.3389/fmars.2016.00118, 2016.

Darby, S. E., Hackney, C. R., Leyland, J., Kummu, M., Lauri, H., Parsons, D. R., Best, J. L., Nicholas, A. P., and Aalto, R.: Fluvial sediment supply to a mega-delta reduced by shifting tropical-cyclone activity, Nature, 539, 276–279, 2016.

DePaolo, D. J. and Wasserburg, G. J.: Nd isotopic variations and petrogenetic models, Geophys. Res. Lett., 3, 249–252, 1976.

Duller, G. A. T.: Distinguishing quartz and feldspar in single grain luminescence measurements, Radiat. Meas., 37, 161–165, 2003.

Farr, T. G., Rosen, P. A., Caro, E., Crippen, R., Duren, R., Hensley, S., Kobrick, M., Paller, M., Rodriguez, E., Roth, L., and Seal, D.: The Shuttle Radar Topography Mission, Rev. Geophys., 45, https://doi.org/10.1029/2005RG000183, 2007.

Fritz, H. M., Blount, C. D., Thwin, S., Thu, M. K., and Chan, N.: Cyclone Nargis storm surge in Myanmar, Nat. Geosci., 2, 448–449, 2009.

Furuichi, T., Win, Z., and Wasson, R. J.: Discharge and suspended sediment transport in the Ayeyarwady River, Myanmar: centennial and decadal changes, Hydrol. Process., 23, 1631–1641, 2009.

Garzanti, E., Wang, J. G., Vezzoli, G., and Limonta, M.: Tracing provenance and sediment fluxes in the Irrawaddy River basin (Myanmar), Chem. Geol., 440, 73–90, 2016.

Gebregiorgis, D., Hathorne, E. C., Sijinkumar, A. V., Nagender Nath, B., Nürnberg, D., and Frank, M.: South Asian summer monsoon variability during the last ∼54 kyrs inferred from surface water salinity and river run off proxies, Quaternary Sci. Rev., 138, 6–15, 2016.

Giosan, L., Constantinescu, S., Clift, P. D., Tabrez, A. R., Danish, M., and Inam, A.: Recent morphodynamics of the Indus delta shore and shelf, Cont. Shelf Res., 26, 1668–1684, 2006.

Giosan, L., Syvitski, J. P. M., Constantinescu, S., and Day, J.: Protect the World's Deltas, Nature, 516, 31–33, 2014.

Giosan, L., Ponton, C., Usman, M., Blusztajn, J., Fuller, D. Q., Galy, V., Haghipour, N., Johnson, J. E., McIntyre, C., Wacker, L., and Eglinton, T. I.: Short communication: Massive erosion in monsoonal central India linked to late Holocene land cover degradation, Earth Surf. Dynam., 5, 781–789, https://doi.org/10.5194/esurf-5-781-2017, 2017.

Godfrey-Smith, D. L., Huntley, D. J., and Chen, W. H.: Optically dating studies of quartz and feldspar sediment extracts, Quaternary Sci. Rev., 7, 373–380, 1988.

Goodbred S. L. and Saito, Y.: Tide dominated deltas, in: Principles of Tidal Sedimentology, edited by: Davis Jr., R. A. and Dalrymple, R. W., 129–49, London: Springer, 2012.

Gordon, R.: Hydraulic work in the Irawadi Delta, Proc. Inst. Civ. Eng., 113, 276–313, 1893.

Hamilton, P. J., O'Nions, R. K., Bridgwater, D., and Nutman, A.: Sm-Nd studies of Archean metasediments and metavolcanics from West Greenland and their implications for the Earth's early history, Earth Planet. Sc. Lett., 62, 263–272, 1983.

Hedley, P. J., Bird, M. I., and Robinson, R. A. J.: Evolution of the Irrawaddy delta region since 1850, Geogr. J., 176, 138–149, 2010.

Hoitink, A. J. F., Wang, Z. B., Vermeulen, B., Huismans, Y., and Kästner, K.: Tidal controls on river delta morphology, Nat. Geosci., 10, 637–645, 2017.

Kars, R. H., Reimann, T., Ankjaergaard, C., and Wallinga, J.: Bleaching of the post-IR IRSL signal: new insights for feldspar luminescence dating, Boreas, 43, 780–791, 2014.

Kravtsova, V. I., Mikhailov, V. N., and Kidyaeva, V. M.: Hydrological regime, morphological features and natural territorial complexes of the Irrawaddy River Delta (Myanmar), Vodn. Resur., 36, 259–276, 2009.

Lambeck, K., Rouby, H., Purcell, A., Sun, Y., and Sambridge, M.: Sea level and global ice volumes from the Last Glacial Maximum to the Holocene, P. Natl. Acad. Sci. USA, 111, 15296–15303, 2014.

Lee, H. Y., Chung, S. L., and Yang, H. M.: Late Cenozoic volcanism in central Myanmar: Geochemical characteristics and geodynamic significance, Lithos, 245, 174–190, 2016.

Liang, M., Kim, W., and Passalacqua, P.: How much subsidence is enough to change the morphology of river deltas?, Geophys. Res. Lett., 43, https://doi.org/10.1002/2016GL070519, 2016.

Licht, A., Reisberg, L., France-Lanord, C., Naing Soe, A., and Jaeger, J. J.: Cenozoic evolution of the central Myanmar drainage system: insights from sediment provenance in the Minbu Sub-Basin, Basin Res., 28, 237–251, 2016.

Liu, C. Z., Chung, S. L., Wu, F. Y., Zhang, C., Xu, Y., Wang, J. G., Chen, Y., and Guo, S.: Tethyan suturing in Southeast Asia: Zircon U-Pb and Hf-O isotopic constraints from Myanmar ophiolites, Geology, 44, 311–314, 2016.

Madsen, A. T., Buylaert, J.-P., and Murray, A. S.: Luminescence dating of young coastal deposits from New Zealand using feldspar, Geochronometria, 38, 378–390, 2011.

Matamin, A. R., Ahmad, F., Mamat, M., Abdullah, K., and Harun, S.: Remote sensing of suspended sediment over Gulf of Martaban, Ekologia, 34, 54–64, 2015.

McHugh, M. G. C., Gurung, D., Giosan, L., Ryan, W. B. F., Mart, Y., Sancar, U., Burckle, L., and Çagatay, M. N.: The last reconnection of the Marmara Sea (Turkey) to the World Ocean: A paleoceanographic and paleoclimatic perspective, Mar. Geol., 255, 64–82, 2008.

McNichol, A. P., Gagnon, A. R., Osborne, E. A., Hutton, D. L., Von Reden, K. F., and Schneider, R. J.: Improvements in procedural blanks at NOSAMS: reflections of improvements in sample preparation and accelerator operation, Radiocarbon, 37, 683–691, 1995.

Milliman, J. D. and Farnsworth, K. L.: River Discharge to the Coastal Ocean: A Global Synthesis, Cambridge Univ. Press, Cambridge, 2010.

Moore E. H.: Early Landscapes of Myanmar, River Books, Bangkok, 272 pp., 2007.

Morley, C. K.: Cenozoic rifting, passive margin development and strike-slip faulting in the Andaman Sea: a discussion of established v. new tectonic models, in: The Andaman–Nicobar Accretionary Ridge: Geology, Tectonics and Hazards, edited by: Bandopadhyay, P. C. and Carter, A., Geological Society, London, Memoirs, 47, 27–50, 2007.

Murray, A. S. and Wintle, A. G.: Luminescence dating of quartz using an improved single-aliquot regenerative-dose protocol, Radiat. Meas., 32, 57–73, 2000.

Murray, A. S., Marten, R., Johnston, A., and Martin, P.: Analysis for naturally occurring radionuclides at environmental concentrations by gamma spectrometry, J. Radioanal. Nucl. Ch., 115, 263–288, 1987.

Murray, A. S., Thomsen, K. J., Masuda, N., Buylaert, J.-P., and Jain, M.: Identifying well-bleached quartz using the different bleaching rates of quartz and feldspar luminescence signals, Radiat. Meas., 47, 688–695, 2012.

Ota, Y., Kawahata, H., Murayama, M., Inoue, M., Yokoyama, Y., Miyairi, Y., Aung, T., Hossain, H. M. Z., Suzuki, A., Kitamura, A., and Moe, K. T.: Effects of intensification of the Indian Summer Monsoon on northern Andaman Sea sediments during the past 700 years, J. Quat. Sci., 32, 528–539, 2017.

Ponton, C., Giosan, L., Eglinton, T., Fuller, D. J., Johnson, E., Kumar, P., and Collet, T. S.: Holocene Aridification of India, Geophys. Res. Lett., 39, L03704, https://doi.org/10.1029/2011GL050722, 2012.

Racey, A. and Ridd, M. F.: Petroleum Geology of Myanmar, Geological Society of London, 2015.

Ramaswamy, V. and Rao, P. S.: The Myanmar continental shelf, in: Continental Shelves of the World: Their Evolution During the Last Glacio-Eustatic Cycle, edited by: Chiocci, F. L. and Chivas, A. R., Bath, UK, Geological Society of London, 231–240, 2014.

Ramaswamy, V., Rao, P. S., Rao, K. H., Thwin, S., Srinivasa Rao, N., and Raiker, V.: Tidal influence on suspended sediment distribution and dispersal in the northern Andaman Sea and Gulf of Martaban, Mar. Geol., 208, 33–42, 2004.

Rao, P. S., Ramaswamy, V., and Thwin, S.: Sediment texture, distribution and transport on the Ayeyarwady continental shelf, Andaman Sea, Mar. Geol., 216, 239–247, 2005.

Reimer P. J., Bard, E., Bayliss, A., Beck, J. W., Blackwell, P. G., Bronk, Ramsey C., Buck, C. E., Edwards, R. L., Friedrich, M., Grootes, P. M., Guilderson, T. P., Haflidason, H., Hajdas, I., Hatté, C., Heaton, T. J., Hoffman, D. L., Hogg, A. G., Hughen, K. A., Kaiser, K. F., Kromer, B., Manning, S. W., Niu, M., Reimer, R. W., Richards, D. A., Scott, M., Southon, J. R., Staff, R. A., Turney, C. S. M., and van der Plicht, J.: IntCal13 and Marine13 radiocarbon age calibration curves 0–50 000 years cal BP, Radiocarbon, 55, 1869–1887, 2013.

Rémillard, A. M., St-Onge, G., Bernatchez, P., Hétu, B., Buylaert, J.-P., Murray, A. S., and Vigneault, B.: Chronology and stratigraphy of the Magdalen Islands archipelago from the last glaciation to the early Holocene: new insights into the glacial and sea-level history of eastern Canada, Boreas, 45, 604–628, 2016.

Rizal, S., Damm, P., Wahid, M. A., Sundermann, J., Ilhamsyah, Y., and Iskandar T.: General circulation in the Malacca Strait and Andaman Sea: A numerical model study, American Journal of Environmental Sciences, 8, 479–488, 2012.

Robinson, R. A. J., Bird, M. I., Oo, N. W., Hoey, T. B., Aye, M. M., Higgitt, D. L., Swe, A., Tun, T., and Win, S. L.: The Irrawaddy river sediment flux to the Indian Ocean: the original nineteenth-century data revisited, J. Geol., 115, 629–640, 2007.

Rodolfo, K. S.: Bathymetry and marine geology of the Andaman Basin, and tectonic implications for Southeast Asia, GSA Bulletin, 80, 1203–1230, 1969a.

Rodolfo, K. S.: Sediments of the Andaman Basin, Northeastern Indian Ocean, Mar. Geol., 7, 371–402, 1969b.

Rodolfo, K. S.: The Irrawaddy Delta: Tertiary setting and modern offshore sedimentation, in: Deltas: Models for Exploration, edited by: Broussard, M. L., Houston Geological Society, Houston, 329–348, 1975.

Scher H. D. and Delaney, M. L.: Braking the glass ceiling for high resolution Nd records in early Cenozoic paleoceanography, Chem. Geol., 269, 269–329, 2010.

Seekins, D. M.: State, society and natural disaster: cyclone Nargis in Myanmar (Burma), Asian J. Soc. Sci., 37, 717–37, 2009.

Shi, W. and Wang, M.: Three-dimensional observations from MODIS and CALIPSO for ocean responses to cyclone Nargis in the Gulf of Martaban, Geophys. Res. Lett., 35, L21603, https://doi.org/10.1029/2008GL035279, 2008.

Stamp, D. L.: The Irrawaddy River, Geogr. J., 5, 329–352, 1940.

Swift, D. J. P. and Thorne, J. A.: Sedimentation on Continental Margins, I: A General Model for Shelf Sedimentation, in: Shelf Sand and Sandstone Bodies: Geometry, Facies and Sequence Stratigraphy, edited by: Swift, D. J. P., Oertel, G. F., Tillman, R. W., and Thorne, J. A., Blackwell Publishing Ltd., Oxford, UK, 1992.

Syvitski, J. P., Kettner, A. J., Overeem, I., Hutton, E. W., Hannon, M. T., Brakenridge, G. R., Day, J., Vörösmarty, C., Saito, Y., Giosan, L., and Nicholls, R. J.: Sinking deltas due to human activities, Nat. Geosci., 2, 681–686, 2009.

Ta, T. K. O., Nguyen, V. L., Tateishi, M., Kobayashi, I., Saito, Y., and Nakamura, T.: Sediment facies and Late Holocene progradation of the Mekong River Delta in Bentre Province, southern Vietnam: an example of evolution from a tide-dominated to a tide-and wave-dominated delta, Sediment. Geol., 152, 313–325, 2002.

Taft, L. and Evers, M.: A review of current and possible future human-water dynamics in Myanmar's river basins, Hydrol. Earth Syst. Sci., 20, 4913–4928, https://doi.org/10.5194/hess-20-4913-2016, 2016.

Tanabe, S., Hori, K., Saito, Y., Haruyama, S., and Kitamura, A.: Song Hong (Red River) delta evolution related to millennium-scale Holocene sea-level changes, Quaternary Sci. Rev., 22, 2345–2361, 2003.

Thomsen, K., Murray, A. S., Jain, M., and Bøtter-Jensen, L.: Laboratory fading rates of various luminescence signals from feldspar-rich sediment extracts, Radiat. Meas., 43, 1474–1486, 2008.

Van der Horst, T.: Sinking Yangon: Detection of subsidence caused by groundwater extraction using SAR interferometry and PSI time-series analysis for Sentinel-1 data, MS Thesis, Delft University of Technology and the National University of Singapore, uuid:8067b72d-94af-44b2-9cb8-5b6c14a8fcde, available at: http://repository.tudelft.nl (last access: 28 May 2018), 2017.

Volker, A.: The deltaic area of the Irrawaddy river in Burma, in Scientific problems of the humid tropical zone deltas and their implications, Proceedings of the Dacca Symposium, UNESCO, 373–379, 1966.

Wang, N., Li, G., Qiao, L., Shi, J., Dong, P., Xu, J., and Ma, Y.: Long-term evolution in the location, propagation, and magnitude of the tidal shear front off the Yellow River Mouth, Cont. Shelf Res., 137, 1–12, 2017.

Woodroffe, C. D., Nicholls, R. J., Saito, Y., Chen, Z., and Goodbred, S. L.: Landscape variability and the response of Asian megadeltas to environmental change. In Global change and integrated coastal management, 277–314, Springer, Dordrecht, 2006.

Xie, S. P., Xu, H., Saji, N. H., Wang, Y., and Liu, W. T.: Role of narrow mountains in large-scale organization of Asian monsoon convection, J. climate, 19, 3420–3429, 2006.